Proceedings of the ASME 2023 International Design Engineering Technical Conferences and Computers and Information in Engineering Conference
IDETC 2023
August 20-23, 2023, Boston, MA, USA

IDETC2023-114907

ROBOTIC EXOSKELETON GLOVE SYSTEM DESIGN AND SIMULATION FOR PATIENTS WITH BRACHIAL PLEXUS INJURIES

Wenda Xu
Robotics and Mechatronics Lab
Mechanical Engineering Department
Virginia Tech,
Blacksburg, Virginia 24061

Yunfei Guo
Robotics and Mechatronics Lab
Electrical and Computer
Engineering department
Virginia Tech,
Blacksburg, Virginia 24061

Pinhas Ben-Tzvi *
Robotics and Mechatronics Lab
Mechanical Engineering Department
Virginia Tech,
Blacksburg, Virginia 24061

ABSTRACT

This paper presents a novel robotic exoskeleton glove system for patients who suffer from brachial plexus injuries. The robotic exoskeleton glove systems takes advantage of our previously designed rigid coupling hybrid mechanism (RCHM) concept that was used for the index finger mechanism design of the exoskeleton glove. The finger mechanism utilizes the single degree of freedom case of the RCHM that combines a rack-and-pinion mechanism and offset-slider-crank mechanism as the rigid coupling mechanism. The serial and special arrangement enables the design of each finger mechanism of the glove with reduced degrees of freedom while more closely imitating the human hand motion. The exoskeleton glove is designed to assist patients with hand disabilities in daily activities, and as such, it is optimized to be compact, lightweight, and portable, and includes modulated electronics for everyday use. The control system contains low-level motor control and high-level human-machine interface components, which enable safe and intuitive control of the exoskeleton glove, thereby enhancing the user's ability to perform various daily activities. A high-level user interface voice activation is also integrated into the system. The paper also describes a simulation environment that was developed using MATLAB Simscape and was designed to test out and optimize different control algorithms.

*Corresponding author – bentzvi@vt.edu

1 INTRODUCTION

The brachial plexus [1] is a critical nerve network that transmits motor and sensory signals to the shoulder, arm, hand, and fingers. Damage to this area can result in loss of muscle control and sensation in the affected limb. Previous research has identified young males as the most common group affected, with causes including traffic accidents, sports injuries, incised wounds, gunshot wounds, carrying heavy backpacks, and inappropriate operative positioning [2]. While surgical interventions can restore shoulder and arm function, restoring mobility and sensation to the wrist and hand is challenging due to the long distance between the injury site and the target nerves [3].

Wearable devices, such as hand exoskeletons, have emerged as a promising tool for improving hand functionality and restoring patients' activities of daily living (ADL). Over the past few decades, numerous robotic rehabilitation hand exoskeletons have been developed, with about half classified as daily assistive tools [4]. Wearable devices offer advantages over stationary devices, as they can be worn for longer periods of time and help patients perform simple ADLs. Previous research has identified several general design requirements for wearable devices [5]. Firstly, the hand mechanism should be compact to avoid collisions with the environment during ADLs. Secondly, the mechanism should be simple for good wearability and the wearer's safety. Thirdly, the ergonomics of the hand exoskeleton, including the remote center of motion (RCM), self-aligning joints, and realizing the natural closing motion of the human finger, are also important for ensuring comfortable operation.

Several wearable hand exoskeleton designs have been pro-

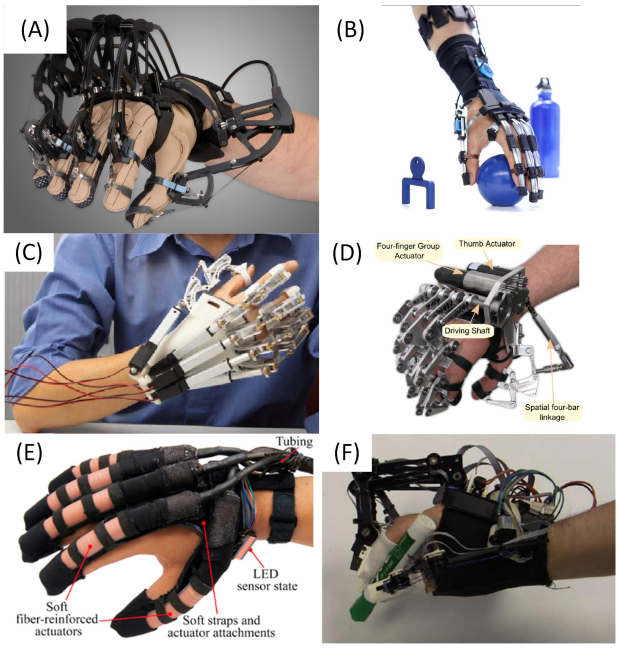

Figure 1. Popular exoskeleton gloves: (A) Cyberglove, (B) Tenoexo, (C) Hope4Care, (D) Bravo, (E) Soft Robotic Glove, (F) Safer. (E) belongs to the soft robotics glove. (C) and (D) belong to the linkage driven glove. (A), (B) and (F) belong to the cable driven / bowden-driven glove.

posed to take advantage of such attributes by employing different approaches as shown in Figure 1. One of the recent and notable approaches that have drawn the attention of researchers is the soft robotic glove [6–9], due to the use of compliant materials, good wearability, low cost, and reduced degrees of freedom. However, these gloves have some limitations, including the use of thick inflatable segments over the fingers to achieve bending motion and the requirement for air compressors and air tanks, which reduces their portability and user mobility.

Similar limitations exist in other robotic gloves driven by hydraulic or pneumatic actuators. Cable-driven and Bowden-driven gloves, such as SAFER [10], CyberGrasp [11], and RAS system [12], utilize a soft glove mechanism without rigid frames to restore hand functionality. However, this design introduces additional issues for the robotic glove, such as uncomfortable pre-tensioning, unexpected shear forces caused by broken cables/tendons, and bulky actuation units mounted on the back of the hand, thereby significantly decreasing the wearability of the glove.

The Bravo [13], and Hope4Care [14] gloves use linkages to transmit motion from the actuators to the hand joints. This design has the advantages of simplicity and compactness but also drawbacks, such as bulkiness and limited range of motion.

To address the limitations of current wearable robotic glove devices, we present a novel exoskeleton glove system with a compact form factor, safe operational functionality, low cost, and user-friendly design. This system integrates an ergonomic finger linkage design, precise force control, and voice activation. We have also developed a simulation environment for future intelligent control training and testing.

The rest of the paper is organized as follows. Section 2 describes the mechanical design of the finger exoskeleton mechanism. Section 3 presents the electronics design of the exoskeleton. Section 4 introduces the control policy of the exoskeleton glove. Section 5 presents the simulation environment and experiments. Section 6 concludes the paper.

2 MECHANISM DESIGN

The exoskeleton glove system is comprised of four finger exoskeletons and a thumb exoskeleton that collectively cover the entire hand. Each finger exoskeleton consists of three links: the distal link, middle link, and proximal link, which correspond to the corresponding phalanges, as well as three relative joints, including the distal interphalangeal (DIP), proximal interphalangeal (PIP), and metacarpophalangeal (MCP) joints. Typically, each joint has one degree of freedom (DOF) for flexion-extension; but the MCP joint possesses an additional DOF for abduction-adduction, which is passively actuated by the thenar eminence. The thumb exoskeleton comprises two distinct links, the distal and proximal links, along with two relative joints, including the interphalangeal (IP) and MCP joints. The carpometacarpal (CMC) joint is designed to emulate human thumb motion.

The motion of different joints on the same exoskeleton linkage are coupled to achieve a compact and lightweight design. Previous research has demonstrated that most grasping motions can be achieved with reduced degrees of freedom in the finger exoskeleton [15–17]. The rigid coupling hybrid mechanism (RCHM) [18] is utilized to couple the motion of different joints.

The main idea of the RCHM is to continuously transfer motion between adjacent links around a joint using a rigid coupling mechanism. The previous research [19] has proved that the rack-pinion and offset-slider-crank mechanisms can be selected as the coupling mechanism for the coupling motion to reduce the size and weight of the exoskeleton glove significantly.

The exoskeleton finger is constructed using offset slider-crank and rack-pinion mechanisms. A linear actuator pushes the output shaft straight forward to create motion. The first offset slider-crank mechanism is composed of the output shaft, the connector, the base, the virtual MCP joint, and the Proximal link. The motion of the output shaft acts as the input, and the reaction of the virtual MCP joint serves as the output. The second offset slider-crank mechanism comprises the base, the connector, the Proximal link, the virtual MCP joint, and the rack. The motion of the virtual MCP joint acts as the input, while the rack serves as the output.

Mimicking the rotation of the MCP joint requires two coupled mechanisms. Through the coupling motion of the pinion-rack mechanism and offset slider-crank mechanism, the linear motion from the linear actuator is transmitted to the linear motion of the first rack in the opposite direction. Furthermore, the remote center of motion mechanism (RCM) avoids interference between the exoskeleton and human fingers. The rotation axis of the RCM is aligned with the MCP joint.

This motion sequence is repeated for the PIP joint, where the other rack on the proximal link drives the joint through the pinion-rack mechanism. The direction of the rack's linear motion changes due to the pinion-rack mechanism. Finally, the motion transmission continues until it reaches the end effector (Distal link).

The forward-motion parts are called the "Driving" chain, as they transmit motion to force the joint to bend. The parts with backward motion are referred to as the "Measuring" chain as they measure the motion of the "Driving" chain and continue to transmit it to the following "Driving" chain. With the alternate motion of the "Driving" and "Measuring" chains, the motion is transmitted to the end of the finger.

In the case of the thumb mechanism design, a similar mechanism is employed to couple the motion of the IP and MCP joints. The CMC joint on the human hand has two DOFs; thus, it is partitioned into two distinct revolute joints on the thumb exoskeleton. One of these joints serves as the active joint that initiates thumb movement, while the other functions as the passive joint designed to track the motion of the thenar eminence in an optimized manner [19].

The entire exoskeleton glove is designed based on the mechanism mentioned above. The overview of the exoskeleton glove is shown in Figure 2. The total weight of each exoskeleton finger is 50 grams.

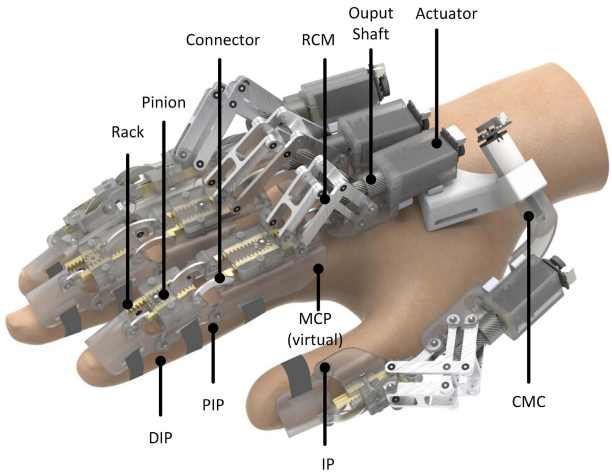

Figure 2. The overview of the exoskeleton glove design. The motion of PIP, DIP, and MCP joints are coupled by the rack-pinion mechanism and offset slider-crank mechanism. The RCM is utilized to substitute the MCP joint for the thenar eminence avoidance.

3 ELECTRONICS DESIGN

The electronics design of the proposed exoskeleton glove is portable and modulated, and all the electronics are embedded in the exoskeleton glove. Since the electronics design is modulated, each part can be easily replaced. No external electrical wiring is required to control the exoskeleton glove. The electronics block diagram is shown in Fig.3. The electronics contain three parts mounted on the forearm of the user.

The first part consists of a battery box that contains three parallel connected 3.7V 1050mAh batteries and a power conversion unit to provide 3V, 5V, and 12V voltage.

The second part consists of a two-piece control unit that contains a Teensy 4.0 microcontroller, an HC-05 Bluetooth unit, and a DVR8801 motor driver. The onboard Teensy 4.0 microcontroller is responsible for sensor reading and performing low-level control, including motor impedance control, motor PID speed control, and motor PID position control. A real-time system is used to minimize the latency of sensor reading and provide the ability for parallel computing. The onboard microcontroller will receive commands from a computer through a Bluetooth connection.

Third, the exoskeleton glove uses seven dual-shaft 12v 1:1000 Pololu metal gear motors to produce sufficient power and torque to generate motion in the proposed exoskeleton glove (one for each finger, one for the thumb thenar, and one for the wrist). Each motor is paired with a DVR-8801 motor driver and 12-CPR magnetic encoders. The motor's electrical current consumption can be measured using the DVR-8801 motor driver. The maximum force that can be generated on each fingertip is 3N.

4 CONTROL SYSTEM DESIGN

The control system of the proposed exoskeleton glove design consists of a low-level motor controller that controls the movement of the electric motors, and a high-level human-machine interface that controls the exoskeleton glove's overall grasp motion.

4.1 Low-Level Motor Control

The proposed exoskeleton glove does not feature any force sensor; thus, it is challenging to control the force. Instead of controlling the force output by the motor or fingertip of the exoskeleton linkages, we control the mechanical impedance of the motor.

The motor's mechanical impedance is measured from the motor's electrical current consumption. When grasping a target

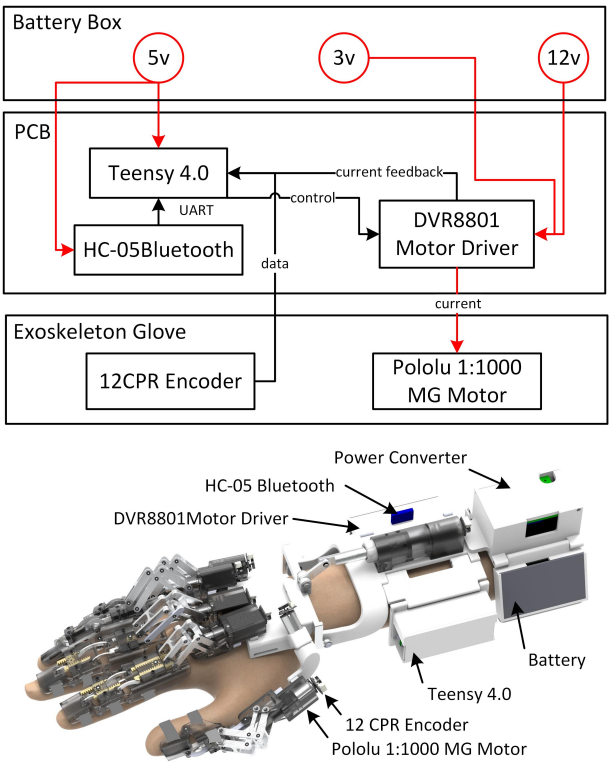

Figure 3. Electronics block diagram.

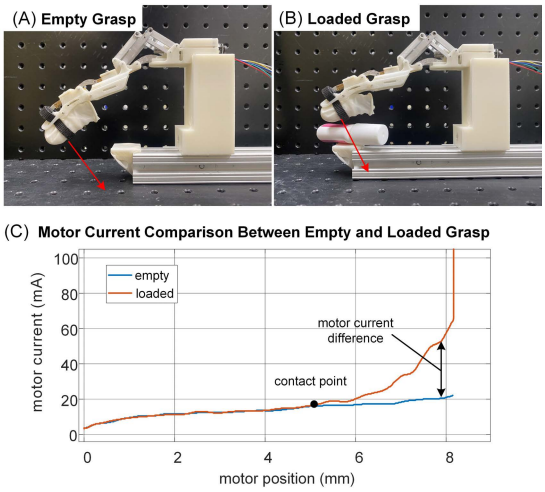

Figure 4. Middle finger mechanism motor's electrical current consumption comparison between unloaded (empty) and loaded grasp.

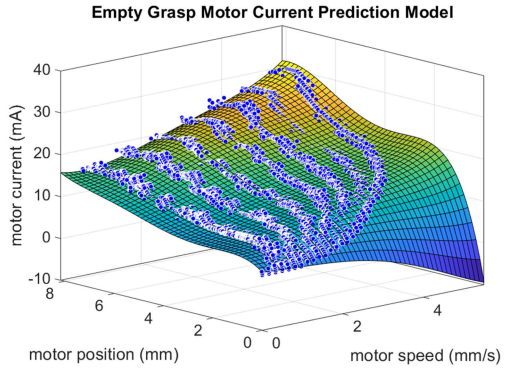

Figure 5. Middle finger mechanism unloaded (empty) grasp motor current prediction model.

object at a constant speed, the object will exert force in the opposite direction to the motor. The motor will consume more electrical current than performing an unloaded (empty) grasp motion to maintain a constant grasp speed. Thus, the mechanical impedance of the motor can be measured by monitoring the motor's electrical current consumption difference between a loaded and unloaded grasp. As an example, the electrical current consumption difference of the middle finger mechanism is shown in Fig.4.

The motor's electrical current consumption difference (I_{diff}) is controlled using Eq.1.

$$I_{diff} = I - I_{pred} \tag{1}$$

where I is the measured current, and I_{pred} is the current consumption during unloaded (empty) grasp. The electrical current consumption for constant grasp speed using the same finger mechanism is repeatable, as shown in Fig.4 (C). Thus, an unloaded (empty) grasp motor current prediction model was designed based on the motor's speed and position to predict I_{pred}. The middle finger mechanism was used to measure the motor's current consumption at seven different speeds in the full position range (motor position starts at 0mm and stops until reaching the mechanical limit) with a sampling rate of 100Hz. Over 8,000 data samples were collected, and over 6,000 data samples were used to build a model using 5^{th} degree linear regression on both the speed and position axes. The model is shown in Fig. 5. The R^2 of the model is 98.8%. 2,000 data samples were reserved for validation; the Mean Absolute Error (MAE) is 1.25mA, and the Mean Absolute Percentage Error (MAPE) is 9.6%.

Therefore, the motor was controlled by monitoring the electric current consumption difference. Although this control method cannot measure the exact motor output force, it can be used to detect contact and the current consumption difference can be used as control feedback to assist grasping. Fig. 7(B) shows the low-level control logic. The motor PID speed controller will move the finger mechanism at a constant speed. The motor current consumption is measured and compared with the no-load motor current consumption. If the motor current consumption difference exceeds a threshold, a motor PID position control is used to lock the motor at the position where current consumption

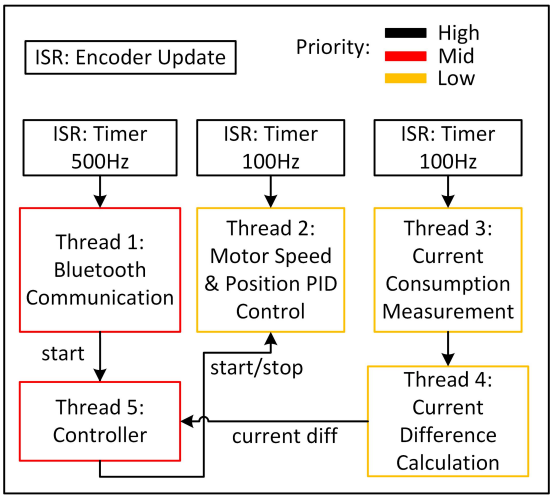

Figure 6. Exoskeleton glove low-level control real-time system structure.

exceeds the threshold value.

The low-level control is implemented on a real-time system following the structure shown in Fig. 6. Threads 2-5 are running in parallel to perform the current consumption control logic. Thread 1 is dedicated for communication with the high-level controller using Bluetooth communication.

4.2 High-Level Human Machine Interface

The high-level controller features a voice-based Human Machine Interface (HMI) called the configurable voice activation and speaker verification system (CVASV) [20, 21]. The key feature of the CVASV system is to provide text-dependent speaker verification for the exoskeleton. Such HMI allowes the user to configure customized activation keywords and provide speaker verification for each input command.

The HMI can convert voice input into grasp type and desired current consumption difference. The exoskeleton can perform six types of grasp, including cylinder grasp, sphere grasp, tip grasp, tripod grasp, lateral grasp, and release. The desired current consumption difference has three levels, including small, medium, and large. Thus, the commands are constructed as [force-level + grasp-type], for example, medium cylinder grasp. Based on experiments, a proper desired current difference was selected for each level and grasp type.

Fig.7(A) shows the high-level controller structure. Voice commands are captured by a wireless microphone and detected by the CVASV system. Desired current difference was set for each motor based on the grasp type and desired current consumption difference level. The expected current difference for each motor is sent to the low-level controller as control input through Bluetooth.

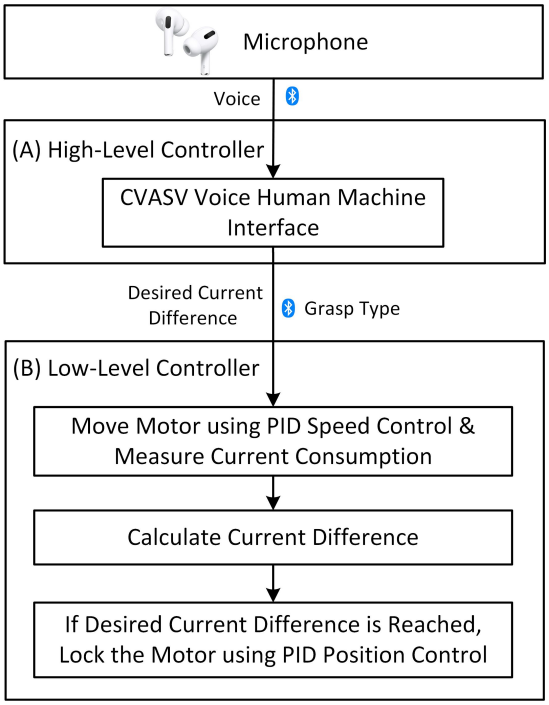

Figure 7. Exoskeleton glove control structure. (A) The CVASV high-level human-machine interface runs on a personal computer or server. CVASV: Configurable voice activation and speaker verification system [20, 21]. (B) Low-level control running on a Teensy 4.0 micro-controller.

5 SIMULATION

Matlab Simscape R2022b was used to simulate the proposed exoskeleton glove. Simulation is a crucial step to ensure hardware and control system proper functioning and is also helpful in accelerating the process of designing complicated control algorithms. The simulation is introduced in the following three parts: (1) simulation parameter selection, (2) control system in the simulation environment, and (3) simulation results.

5.1 Simulation Parameter Selection

Three sets of parameters are essential for a simulation to function correctly.

The first set of parameters is the physical parameters of the simulated object, such as the mass, center of mass, and momentum of inertia. In our simulation, the material property was set in SolidWorks and automatically generated the above parameters. Fig. 8(A) shows the simulated index finger with assigned materials.

The second set of parameters is the internal mechanism of the simulated actuators. In the real world, the proposed exoskeleton contains seven actuators: one for each finger, one for the thumb thenar, and one for the wrist. Passive revolute joints were

used between the finger mechanism and exoskeleton glove base to adapt a human finger's abduction and abduction motion. The passive joints are shown in Fig. 8(B) labeled as revolute joint A. However, in simulation, these revolute joints are treated as actuators in order to reduce the computational cost of the simulation. In this way, the simulation does not need to calculate the contact force between the finger mechanisms and fingers. Thus, each finger consists of two actuators, one prismatic joint to control the linear motion of the finger mechanism and one revolute joint to simulate a human finger's abduction and adduction motions. In addition to the ten actuators, which control the finger mechanism, there is the revolute joint B for the thumb thenar's rotary motion. Two more actuators control the wrist motion to simulate a human wearing the exoskeleton glove. These actuators are labeled in Fig. 8(B). For the simulated actuators that do not match an actual hardware actuator, we control the position of the actuator. Aspring-damper system was set up as the actuator's internal mechanism for the simulated actuators representing a motor in the actual hardware. The spring-damper system for the prismatic joints has a spring stiffness of 300 N·m, a damping ratio of 100 N·m/s, and the revolute joint B has a spring stiffness of 300 N·deg and a damping ratio of 100 N·deg/s. These values were selected based on a trial and error process in order to match with the hardware.

The third set of parameters is the contact force calculation parameters. In this case, the contact between the finger and the target object was of concern in order to achieve faster simulation speed. The contact force parameters include stiffness, damping ratio, and static and dynamic friction. These parameters were acquired from previous research [22].

5.2 Control System

The control logic for the simulated actuators is discussed in this section. For the simulated actuators that do not match an actual hardware actuator, the position of the actuator was controlled using the built-in position controller.

The control logic shown in Fig. 9(A) was used for the simulated actuators that correspond to an actual hardware actuator. The logic is similar to what we used to control the actuator described in Fig. 7(B). The control input is the desired force, and PID speed control is performed when the measured force does not exceed the desired force. If the measured force exceedsthe desired force, a PID position control is used to lock the actuator in place. Fig. 9(B) shows a simulated actuator's measured force and position while grasping a target object. The desired force is 20 N, and the actuator is locked at around 9.5 mm.

5.3 Simulation Results

A simulation was performed with the previously discussed simulation parameters and control algorithm, and the result is shown in Fig. 10. The target object is a simulated 500 ml plastic

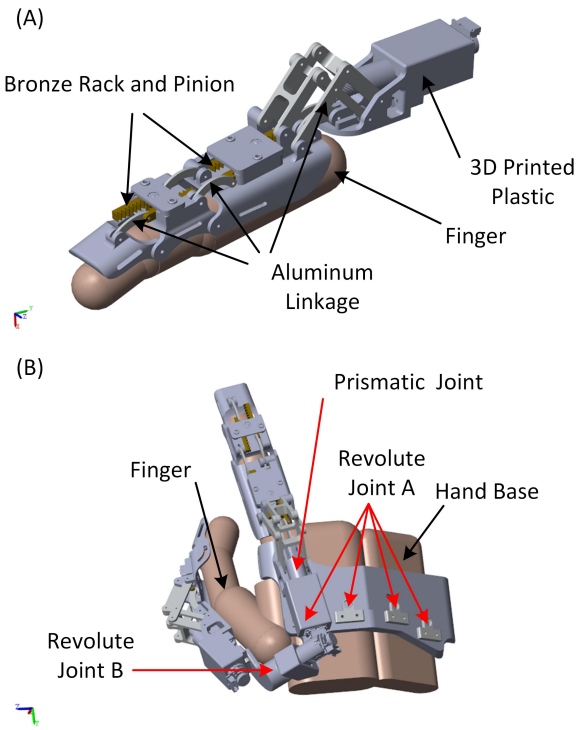

Figure 8. Simulated exoskeleton glove. (A) Simulated index finger with labeled material. (B) Simulated two-finger exoskeleton glove with labeled actuators.

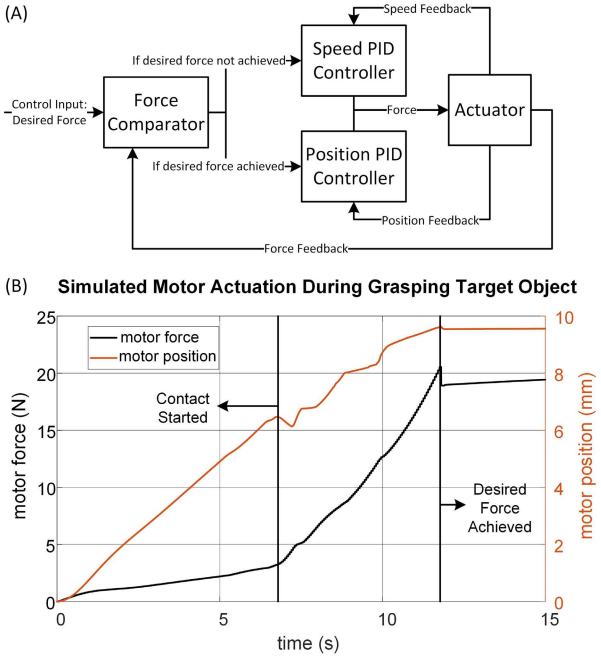

Figure 9. (A) Simulated finger mechanism actuator control structure. (B) Simulated finger mechanism actuator's measured force and position during grasping a target object.

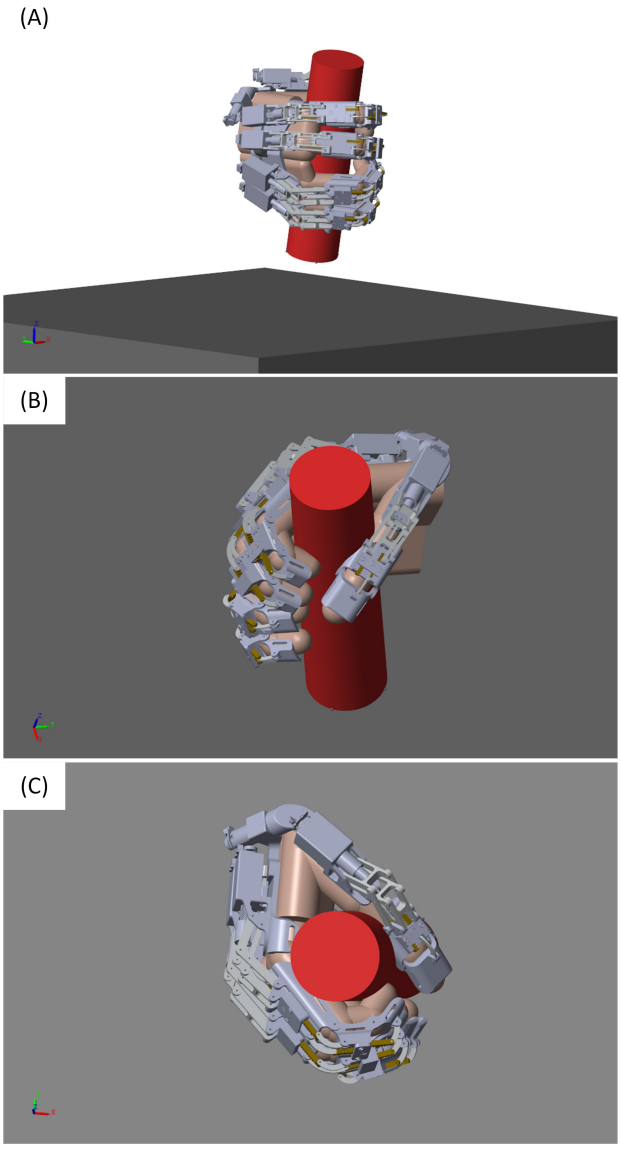

Figure 10. Simulation result of the purposed exoskeleton glove grasp grasping a 500 ml plastic water bottle. (A) Side view of the exoskeleton glove. (B) 45-degree angled view of the exoskeleton glove. (C) Top view of the exoskeleton glove.

water bottle full of water. The exoskeleton successfully grasps and lifts the target object, which proves the appropriateness and accuracy of the design, control algorithm, and simulation environment.

6 CONCLUSION

In this paper, an exoskeleton glove system was presented for individuals with hand disabilities to assist with their activities of daily living and for rehabilitation. The mechanical design and electronics design of the exoskeleton glove were presented first. The mechanical design focused on creating a lightweight, comfortable glove that provides assistance and support to the user's hand. The electronics design focused on portability and modularity for daily use. The control system design was also presented, which consisted of a low-level motor control and high-level human machine interface. In addition, a simulation environment setup was designed and introduced for basic experiments with the purpose of demonstrating that our proposed system can grasp, and also to serve as a tool for testing other intelligent control methods in the future.

The control system design was an essential component of the project, as it allowed for the efficient and effective operation of the exoskeleton glove. The low-level motor control system ensured that the motors operated correctly and safely. At the same time, the high-level human-machine interface allowed the user to easily control the glove and customize its behavior to their individual needs.

To evaluate the performance of the exoskeleton glove system and to be able to develop intelligent control methods in the future, a simulation environment was designed, and basic experiments were conducted. The results demonstrated that the proposed system has the ability to grasp objects and perform intelligent control, paving the way for further development and improvements. Overall, this exoskeleton glove system has the potential to significantly improve the quality of life for individuals with hand disabilities, providing them with increased independence and autonomy in their daily activities.

In order to further enhance the effectiveness and precision of the low-level control method proposed, future work should focus on addressing two key aspects. First, it is crucial to investigate and establish a clear relationship between the motor's output force and its current consumption through extensive experiments. This empirical data will provide valuable insights into effectively controlling and regulating the motor's output force. Second, the grasp force utilized in the simulation experiments was determined through trial and error. To overcome the limitations of this approach and ensure robust control, future efforts should be directed towards designing a more sophisticated control policy. This can be achieved by leveraging the advantages of a simulation environment, which offers a controlled and flexible platform for iterative testing and optimization. By systematically exploring different control strategies within the simulation, a robust and efficient control policy can be developed, enabling more accurate and reliable grasp force manipulation.

ACKNOWLEDGMENT

Research reported in this publication was supported in part by the Eunice Kennedy Shriver National Institute of Child Health & Human Development of the National Institutes of Health under Award Number R21HD095027. The content is solely the

responsibility of the authors and does not necessarily represent the official views of the National Institutes of Health. This material is partly based upon work supported by (while serving at) the National Science Foundation.

REFERENCES

[1] Midha, R., 1997. "Epidemiology of Brachial Plexus Injuries in a Multitrauma Population". *Neurosurgery*(June), pp. 1182–1189.

[2] Park, H. R., Lee, G. S., Kim, I. S., and Chang, J.-C., 2017. "Brachial Plexus Injury in Adults". *The Nerve,* ***3***(1), pp. 1–11.

[3] Giuffre, J. L., Kakar, S., Bishop, A. T., Spinner, R. J., and Shin, A. Y., 2010. "Current Concepts of the Treatment of Adult Brachial Plexus Injuries". *Journal of Hand Surgery,* ***35***(4), 4, pp. 678–688.

[4] Ferguson, P. W., Shen, Y., and Rosen, J., 2019. *Hand exoskeleton systems-overview*. INC.

[5] Iqbal, J., Tsagarakis, N. G., Fiorilla, A. E., and Caldwell, D. G., 2009. Design requirements of a hand exoskeleton robotic device. Tech. rep.

[6] Polygerinos, P., Wang, Z., Galloway, K. C., Wood, R. J., and Walsh, C. J., 2015. "Soft robotic glove for combined assistance and at-home rehabilitation". *Robotics and Autonomous Systems,* ***73***, pp. 135–143.

[7] Deimel, R., and Brock, O., 2016. "A novel type of compliant and underactuated robotic hand for dexterous grasping". *The International Journal of Robotics Research,* ***35***(1-3), 1, pp. 161–185.

[8] Ilievski, F., Mazzeo, A. D., Shepherd, R. F., Chen, X., and Whitesides, G. M., 2011. "Soft Robotics for Chemists". *Angewandte Chemie,* ***123***(8), 2, pp. 1930–1935.

[9] Yap, H. K., Ang, B. W., Lim, J. H., Goh, J. C., and Yeow, C. H., 2016. "A fabric-regulated soft robotic glove with user intent detection using EMG and RFID for hand assistive application". In Proceedings - IEEE International Conference on Robotics and Automation, Vol. 2016-June, Institute of Electrical and Electronics Engineers Inc., pp. 3537–3542.

[10] Ma, Z., Ben-Tzvi, P., and Danoff, J., 2015. "Sensing and Force-Feedback Exoskeleton Robotic (SAFER) Glove Mechanism for Hand Rehabilitation". *Proceedings of the ASME Design Engineering Technical Conference,* ***5A-2015***, pp. 1–8.

[11] Aiple, M., and Schiele, A., 2013. "Pushing the limits of the CyberGrasp™ for haptic rendering". *Proceedings - IEEE International Conference on Robotics and Automation*, pp. 3541–3546.

[12] Hofmann, U. A., Bützer, T., Lambercy, O., and Gassert, R., 2018. "Design and Evaluation of a Bowden-Cable-Based Remote Actuation System for Wearable Robotics". *IEEE Robotics and Automation Letters,* ***3***(3), pp. 2101–2108.

[13] Leonardis, D., Barsotti, M., Loconsole, C., Solazzi, M., Troncossi, M., Mazzotti, C., Castelli, V. P., Procopio, C., Lamola, G., Chisari, C., Bergamasco, M., and Frisoli, A., 2015. "An EMG-controlled robotic hand exoskeleton for bilateral rehabilitation". *IEEE Transactions on Haptics,* ***8***(2), pp. 140–151.

[14] Ho, N. S., Tong, K. Y., Hu, X. L., Fung, K. L., Wei, X. J., Rong, W., and Susanto, E. A., 2011. "An EMG-driven exoskeleton hand robotic training device on chronic stroke subjects: Task training system for stroke rehabilitation". In IEEE International Conference on Rehabilitation Robotics.

[15] Ma, Z., Ben-Tzvi, P., and Danoff, J., 2016. "Hand Rehabilitation Learning System with an Exoskeleton Robotic Glove". *IEEE Transactions on Neural Systems and Rehabilitation Engineering,* ***24***(12), pp. 1323–1332.

[16] Refour, E., Sebastian, B., and Ben-Tzvi, P., 2017. "Design and integration of a two-digit exoskeleton glove". In Proceedings of the ASME Design Engineering Technical Conference, Vol. 5A-2017, pp. 1–8.

[17] Bekey, G. A., Tomovic, R., and Zeljkovic, I., 1990. "Control Architecture for the Belgrade/USC Hand". *Dextrous Robot Hands*, pp. 136–149.

[18] Liu, Y., and Ben-Tzvi, P., 2020. "Design, Analysis, and Integration of a New Two-Degree-of-Freedom Articulated Multi-Link Robotic Tail Mechanism". *Journal of Mechanisms and Robotics,* ***12***(2), pp. 1–9.

[19] Xu, W., Liu, Y., and Ben-Tzvi, P., 2022. "Development of a novel low-profile robotic exoskeleton glove for patients with brachial plexus injuries". In 2022 IEEE/RSJ International Conference on Intelligent Robots and Systems (IROS), IEEE, pp. 11121–11126.

[20] Guo, Y., Xu, W., Pradhan, S., Bravo, C., and Ben-Tzvi, P., 2020. "Integrated and configurable voice activation and speaker verification system for a robotic exoskeleton glove". In Proceedings of the ASME Design Engineering Technical Conference, Vol. 10, p. Under Review.

[21] Guo, Y., Xu, W., Pradhan, S., Bravo, C., and Ben-Tzvi, P., 2022. "Personalized voice activated grasping system for a robotic exoskeleton glove". *Mechatronics,* ***83***, p. 102745.

[22] Park, J., Pažin, N., Friedman, J., Zatsiorsky, V. M., and Latash, M. L., 2014. "Mechanical properties of the human hand digits: Age-related differences". *Clinical Biomechanics,* ***29***(2), pp. 129–137.